Slow Heterogeneous Charge Transfer Kinetics for the ClO_2^-/ClO_2 Redox Couple at Platinum, Gold, and Carbon Electrodes. Evidence for Nonadiabatic Electron Transfer

Namphol Sinkaset, Akane M. Nishimura, Josh A. Pihl, and William C. Trogler*

Department of Chemistry and Biochemistry, University of California at San Diego, La Jolla, California 92093-0358

Received: July 30, 1999; In Final Form: October 7, 1999

Chlorite (ClO_2^-) is one of the few simple aqueous anions that forms a stable product on one-electron oxidation. The heterogeneous charge transfer rate constants at $E° = 0.700$ V vs SCE for the ClO_2^-/ClO_2 redox couple have been measured at Au, Pt, and glassy carbon electrodes in aqueous KNO_3 solutions using rotating disk and ac voltammetry techniques between 10 and 30 °C. At 25 °C in 1.0 M KNO_3 and pH = 7, the standard heterogeneous rate constants k_{el} were measured as 0.015 ± 0.001 cm/s and 0.014 ± 0.003 cm/s, respectively, at Au and reduced Pt electrodes. The transfer coefficient α on gold was measured to be 0.50 ± 0.01 using ac voltammetry. The heterogeneous rate constants obtained with the use of a glassy carbon electrode were slower (0.0079 ± 0.001 cm/s at 25 °C). The measured activation free energy for electron transfer at a gold electrode was 25 ± 3.3 kJ/mol with a preexponential factor of $310(+900/-230)$ cm/s. Heterogeneous rate constants of experiments performed in D_2O solvent were only slightly slower than those measured in H_2O, indicating that the redox couple does not exhibit differential hydrogen bonding. Digital simulation of cyclic voltammograms, with k_{el} determined from the ac voltammetry and rotating disk techniques, gave good agreement with experiment. Marcus theory was applied to understand the unexpected slow heterogeneous kinetics for this simple redox couple. Additionally, the preexponential factor in the semiclassical expression describing heterogeneous electron transfer was examined. The slow electron transfer process is primarily attributed to a small preexponential factor that may arise from a high degree of nonadiabaticity in the electron transfer process.

Introduction

Interest has grown in using chlorine dioxide (ClO_2) as a disinfectant in municipal water supplies because it reduces the trihalomethane products observed in conventional chlorine water treatment.[1−8] Chlorine dioxide has also been employed as a disinfectant in the food service industry and hospitals.[9−14] Its widespread use in the paper industry as an alternative to chlorine pulp bleaching has greatly reduced formation of chlorinated dioxins.[15−17] The greater effectiveness of ClO_2 against certain bacteria, including *Cryptosporidium parvum*, makes it an attractive alternative to conventional chlorine disinfection of drinking water.[18,19] The photochemistry of ClO_2 in aqueous solution has been studied, and it has been suggested that stratospheric ClO_2, formed by the reaction between BrO and ClO, could photochemically generate Cl radicals and cause catalytic destruction of ozone.[20]

Despite its increased use, the kinetics of secondary reactions involving chlorine dioxide have not received much attention. Previous studies of chlorine dioxide reaction kinetics employed stock solutions and monitored changes in the UV/vis spectrum.[21−24] This method suffers from disadvantages ranging from the purity of ClO_2 stock solutions to the formation of colored adducts between ClO_2 and certain nucleophiles.[8,21] In contrast, transient electrochemical techniques, such as cyclic voltammetry, offer the advantage of providing pure ClO_2 at the instant the experiment is being performed, and reactivities with other compounds can also be studied by time dependent techniques.

The availability of commercial ClO_2 generating systems that form chlorine dioxide electrochemically suggested that chlorine dioxide would be amenable to mechanistic electrochemical study. It can be cleanly produced by electrochemical oxidation of the chlorite (ClO_2^-) anion. Surprisingly, few electrochemical kinetic studies have examined the oxidation of chlorite to form chlorine dioxide. Diffusion coefficients have been measured using rotating disk electrochemistry, but complications were encountered when platinum electrodes were used.[25] Several electrochemical studies of ClO_2^- have been focused on analytical detection limits.[8,26−28]

Before the reactivity between chlorine dioxide and other solution components can be studied electrochemically, the electron transfer kinetics of the ClO_2^-/ClO_2 couple must be understood. Heterogeneous rate parameters can then be used in digital simulations involving electrochemically generated chlorine dioxide. In the present work, the heterogeneous charge transfer kinetics of the ClO_2^-/ClO_2 redox couple were investigated on Au, Pt, and glassy carbon electrodes in KNO_3 solutions using rotating disk methods and ac voltammetry. Additionally, Marcus theory was applied to gain insight into the factors influencing the slow heterogeneous charge transfer kinetics of the ClO_2^-/ClO_2 redox couple.

Experimental Section

Materials. Supporting electrolyte (KNO_3, Certified ACS, Fisher) was recrystallized from HPLC grade water (Fisher). Water purified by a Millipore Milli-Q system was used for all electrochemical solutions. D_2O (99.9 atom % D, Aldrich) was used as received. $NaClO_2$ (technical 80%, Aldrich) was recrystallized from 75% acetone/water followed by a second recrys-

10.1021/jp992693f CCC: $18.00
Published on Web 11/18/1999

tallization from 70% acetonitrile/water. The recrystallized $NaClO_2$ was dried under vacuum overnight and stored under an Ar atmosphere in a Schlenk flask wrapped in aluminum foil to prevent photodecomposition. The purity of $NaClO_2$ was monitored with a Hewlett-Packard 8452A diode array spectrometer in 1.0 cm quartz cells, using the 262 nm absorption with an extinction coefficient $\epsilon = 140\ M^{-1}\ cm^{-1}$.[21]

Apparatus. Cyclic, ac, and rotating disk voltammograms were obtained using a Bioanalytical Systems (BAS) 100 Electrochemical Analyzer. For the rotating disk experiments, a Pine Instrument Company Analytical Rotator Model MSR was used to control the rotation rate. Data were transferred from the BAS 100 to a Hewlett-Packard Vectra Pentium computer. Microsoft Excel was used to analyze the data and generate the voltammograms. Digital simulation was carried out on the Hewlett-Packard Vectra Pentium system using the DigiSim software package v. 2.1 available from BAS. Molecular modeling of ClO_2^- was accomplished using Hyperchem 5.1 Pro for Windows, available from Hypercube, Inc.

Au, Pt, and glassy carbon rotating disk electrodes (geometric area 0.1963 cm^2) obtained from Pine instruments were used for all experiments. Metal working electrodes were rinsed with concentrated HNO_3 (Certified ACS Plus, Fisher) and polished on microcloth polishing pads (Bioanalytical Systems) successively with slurries of 220, 320, 400, and 600 grit polish to obtain a mirror finish. The electrodes were rinsed with HPLC grade water between each polishing. The glassy carbon electrode was polished using HPLC grade water. A saturated calomel electrode was used as the reference electrode, and a Pt coil was used as the auxiliary electrode. Experiments were carried out in a custom glass cell with a thermostated jacket. An Endocal constant temperature recirculating bath was used to maintain the cell temperature. The solution temperature was measured directly with a mercury thermometer.

Experiments were performed at pH values of 5, 6, and 8 to determine whether proton concentration had an appreciable affect on k_{el}. The pH of the 1.0 M KNO_3 supporting electrolyte was adjusted by adding either concentrated HNO_3 or 2.0 M NaOH while monitoring with a pH meter (Accumet AB15, Fisher). At lower pH, the heterogeneous charge transfer rate constants at a gold electrode were slower ($k_{el} = 0.012 \pm 0.001$ cm/s at pH 5), but no deviation was observed at higher pH. The pK_a of ClO_2^- is 1.96.[21] Because the effect of proton concentration above the pK_a was small, measurements were taken at neutral pH.

In a typical electrochemical experiment, 20.0 mL of a 1.0 M KNO_3 stock solution was placed in the electrochemical cell. The chosen rotating disk electrode and the Pt coil auxiliary electrode were washed with HNO_3 (unless it was glassy carbon) and polished. The rotating disk electrode was assembled and immersed in the solution along with the Pt coil auxiliary electrode and SCE. The thermometer was placed in solution, as well as a custom-made glass sparge. The recirculating bath was set to the appropriate temperature, and Ar gas (99.997%, Parsons) was bubbled into the solution for at least 15 min before each experiment. After the solution reached the desired temperature, the glass sparge was raised above the solution, and the Ar flow was continued to blanket the solution. A background cyclic voltammogram of the supporting electrolyte was measured before each experiment. Then, 0.0090 g of $NaClO_2$ was added to the solution and dissolved by rotating the working electrode. A cyclic voltammogram was recorded to ensure that a clean, reversible ClO_2^-/ClO_2 couple was observed. In the case of the Pt electrode, electrochemical pretreatment (hydrogen gas evolution at -2.0 V vs SCE for 10 s before each scan) was required to obtain reproducible rotating disk voltammograms.

Diffusion coefficients of ClO_2^- as a function of temperature were derived from Levich plots[29] obtained with a rotating Au disk electrode. Kinematic viscosities of the 1.0 M KNO_3 supporting electrolyte were measured with the use of a Cannon-Fenske routine size 25 viscometer (Fisher) immersed in a thermostated bath. The refractive index of 1.0 M KNO_3 was measured using a Bausch and Lomb refractometer.

Electrochemical Measurements. The method for determining k_{el}, the standard electrochemical rate constant, by rotating disk electrochemistry is described by Bard and Faulkner.[29] At each temperature, cyclic voltammograms were taken to determine the $E_{1/2}$ for the ClO_2^-/ClO_2 couple (0.700 ± 0.004 V vs SCE). Rotating disk voltammograms were obtained at 600, 1000, 2000, 3000, and 4000 rpm. Capacitive currents were manually subtracted by extrapolating the baseline of the voltammogram to obtain the true faradaic current.

The ac voltammograms were collected with a gold electrode. At each temperature, cyclic voltammograms at 50 mV/s were taken to determine the $E_{1/2}$ for the ClO_2^-/ClO_2 couple (0.700 ± 0.004 V vs SCE). The solution resistance, R_u, was measured at a potential 500 mV removed from $E_{1/2}$. The double-layer capacitance was determined by the procedure outlined by Smith.[30] The necessary frequency of the sinusoidal excitation was estimated using eq 1, where ω is the angular frequency of the sinusoidal voltage ($2\pi f$) and D is the diffusion coefficient of the electroactive species.[31] The approximate k_{el} was determined from the peak separation obtained from the cyclic voltammogram.[29]

$$k_{el} \ll (\omega D)^{1/2} \tag{1}$$

Phase selective ac voltammograms were taken at this frequency, and the in-phase and 90° out-of-phase ac voltammograms were used to plot cot ϕ vs the applied linear potential. To correct for double-layer capacitance and solution resistance, the experiment was repeated in the absence of the redox couple being studied. Vector subtraction, as described by Smith,[30] was then used to obtain the true heterogeneous charge transfer rate constant.

Double potential step chronocoulometry was performed using the BAS 100. Anson plots[29] were also generated with this instrument to see if significant adsorption was occurring.

Results and Data Analyses

Behavior of the ClO_2^-/ClO_2 Redox Couple at a Pt Electrode. Commercial sodium chlorite is only of 80% purity, and it was crucial to obtain purified material that exhibits a low background current necessary for quantitative electrochemical study. Successive recrystallizations from 75% acetone/water and 70% acetonitrile/water provided pure $NaClO_2$ suitable for electrochemical measurements. The ClO_2^-/ClO_2 redox couple was examined initially using cyclic voltammetry at a Pt electrode. It was discovered that electrode history and pretreatment greatly affected the reproducibility of the electrochemical scans. If no pretreatment scheme was applied, the ClO_2^-/ClO_2 wave broadened gradually over time. However, if the electrode was pretreated by holding the potential at -2.0 V vs SCE to induce vigorous hydrogen evolution for 10 s before each scan, then clean, chemically reversible waves were consistently observed (Figure 1). If the electrode was pretreated by holding the potential at 0.10 V vs SCE for 1 min with a 1000 rpm

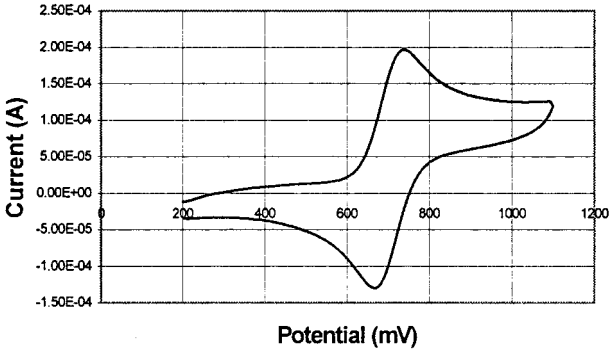

Figure 1. Cyclic voltammogram of 5.0 mM $NaClO_2$ in 1.0 M KNO_3 at a reduced Pt electrode at 25 °C, scan rate = 50 mV/s (vs SCE).

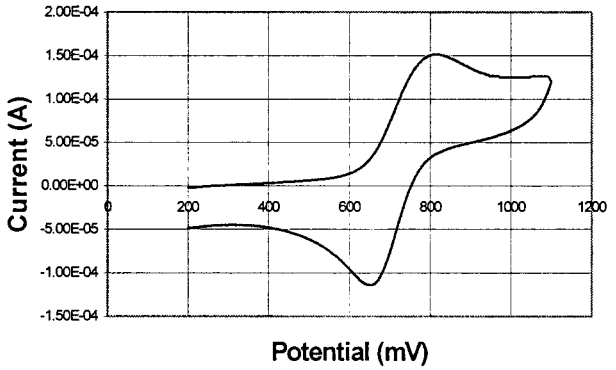

Figure 2. Cyclic voltammogram of 5.0 mM $NaClO_2$ in 1.0 M KNO_3 at a surface-fouled Pt electrode at 25 °C, scan rate = 50 mV/s (vs SCE).

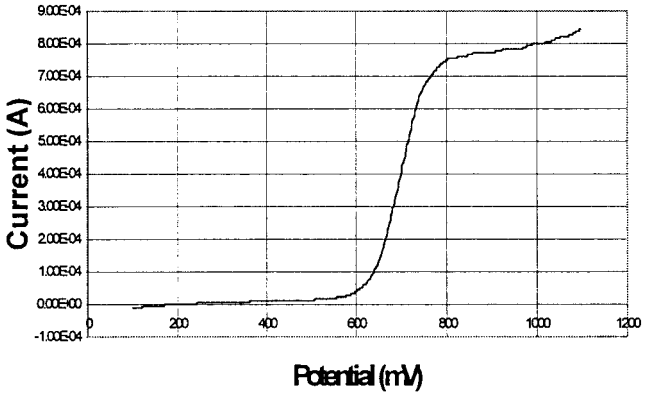

Figure 3. Rotating disk voltammogram at a Au electrode of 5.2 mM $NaClO_2$ in 1.0 M KNO_3 at 25 °C, 1000 rpm, scan rate = 100 mV/s (vs SCE).

rotation rate, a broadened ClO_2^-/ClO_2 wave was observed as shown in Figure 2. It is possible that this latter pretreatment scheme results in hydrogen adsorption.[32] The increased peak separation is indicative of sluggish electron transfer kinetics.[29] The rate of electron transfer was determined on a reduced Pt surface by rotating disk electrochemistry. The electron transfer rate at 25 °C was 0.014 ± 0.003 cm/s. However, on the other Pt surface, the rate falls to 0.0030 ± 0.0007 cm/s. This observation may be significant since some industrial processes (e.g., Sterling Chemicals ECF system) employ platinized titanium electrodes in bulk preparations of ClO_2.

Heterogeneous Charge Transfer Rate Constants for the ClO_2^-/ClO_2 Redox Couple at a Gold Electrode. Since Au is less prone to surface fouling, heterogeneous rate constants were primarily obtained with this electrode. Two independent methods, rotating disk and ac voltammetry, were used to determine

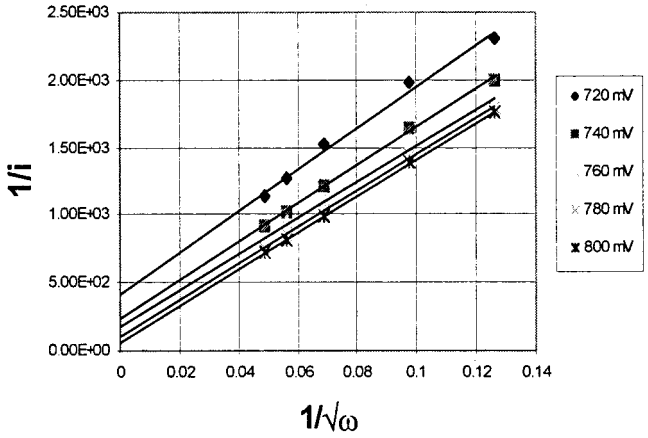

Figure 4. Extrapolation of $1/i$ to infinite rotation rate at five overpotentials (vs SCE). Au electrode, 5.2 mM $NaClO_2$ in 1.0 M KNO_3, 25 °C.

TABLE 1: Heterogeneous Charge Transfer Rate Parameters for ClO_2^-/ClO_2 in 1.0 M KNO_3 as a Function of Temperature Obtained from Rotating Disk Voltammograms on a Au Electrode

T (K)	k_{el} (cm/s)	α
283	0.0098 ± 0.0005	0.56 ± 0.02
288	0.010 ± 0.0004	0.56 ± 0.02
293	0.013 ± 0.0009	0.57 ± 0.03
298	0.015 ± 0.001	0.63 ± 0.03
303	0.019 ± 0.003	0.61 ± 0.05

the rate of electron transfer. Rotating disk voltammograms were taken at 600, 1000, 2000, 3000, and 4000 rpm. A sample voltammogram is shown in Figure 3. Plots of $1/i$ vs $1/(\omega)^{1/2}$ were used to determine the current at infinite rotation rate at five different overpotentials, as shown in Figure 4. The current at infinite rotation rate i_k is related to the rate of electron transfer by eq 2, where n = no. of electrons, F = Faraday's constant, A = electrode area in cm^2, k_f = electron transfer rate, and C_R^* = concentration in mol/cm^3.

$$i_k = nFAk_fC_R^* \tag{2}$$

Heterogeneous rates as a function of five different overpotentials were used to generate plots of ln k_f vs η (overpotential). This plot was extrapolated to zero overpotential to determine k_{el}. Additionally, the transfer coefficient α can be determined from this plot using the relation in eq 3, where m = slope, R = ideal gas constant, and T = temperature in K.

$$m = \alpha n\frac{F}{RT} \tag{3}$$

Measurements were taken between 10 and 30 °C in 5 °C increments (Table 1). The standard heterogeneous rate constant is related to the free energy of activation by eq 4, the semiclassical equation for heterogeneous electron transfer, where δr = reaction zone thickness, κ_{el}^0 = electronic transmission coefficient at distance of closest approach, ν_n = nuclear frequency factor, and Γ_n = nuclear tunneling factor.[33]

$$k_{el} = \delta r\, \kappa_{el}^0 \nu_n \Gamma_n \exp\left(\frac{-\Delta G^{\ddagger}}{RT}\right) \tag{4}$$

A plot of ln k_{el} vs $1/T$ (Figure 5) yields an activation free energy of 25 ± 3.3 kJ/mol and a preexponential factor of 310-(+900/−230) cm/s.

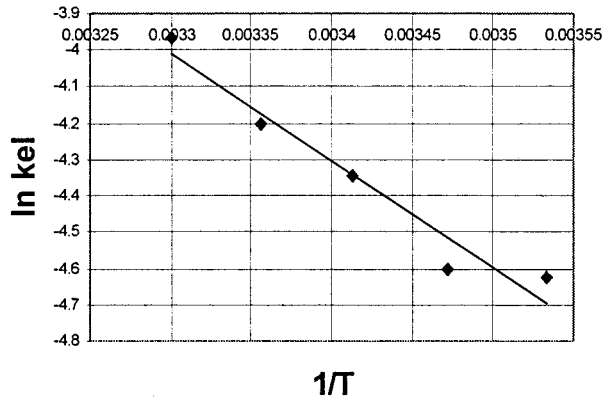

Figure 5. Plot of ln k_{el} vs $1/T$ for the ClO_2^-/ClO_2 redox couple at a rotating disk Au electrode.

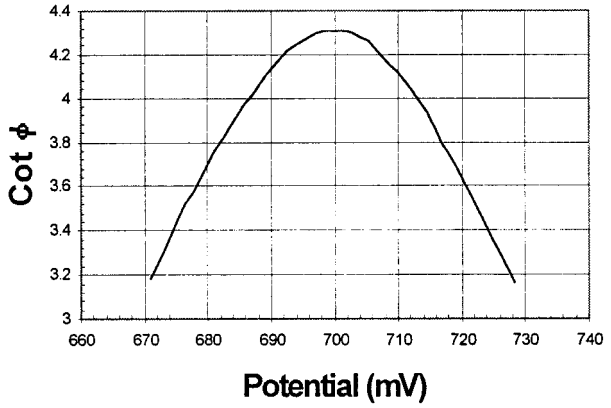

Figure 6. Plot of cot ϕ vs applied linear potential from ac voltammograms of 5.0 mM $NaClO_2$ in 1.0 M KNO_3 at a Au electrode at 25 °C, $f = 105$ Hz, $\Delta E = 25$ mV (vs SCE).

The determination of heterogeneous charge transfer rate constants by ac voltammetry is cited to be very accurate.[29] One of the advantages of ac voltammetry is that the double-layer capacitance and solution resistance can be separated from the faradaic response in the rate constant calculation. A series of ac voltammograms were taken at different phase angles to determine the in-phase response. The in-phase and 90° out-of-phase ac voltammograms were recorded and used to plot cot ϕ vs the applied linear potential. An example of this plot is shown in Figure 6. From this plot, α and k_{el} can be determined from eq 5 and eq 6, where E_{dc} = potential at $[\cot \phi]_{max}$.

$$E_{dc} = E_{1/2} + \frac{RT}{nF}\ln\left(\frac{\alpha}{1-\alpha}\right) \quad (5)$$

$$[\cot \phi]_{max} = 1 + \frac{[2D_R^{(1-\alpha)} D_O^{\alpha} \omega]^{1/2}}{\alpha^{-\alpha}(1-\alpha)^{-(1-\alpha)} k_{el}} \quad (6)$$

The required diffusion coefficients were taken from Levich plots obtained from rotating disk electrochemical data for ClO_2^-. The diffusion coefficients of ClO_2^- and ClO_2 were assumed to be identical. The measured kinematic viscosities of the 1.0 M KNO_3 solution, as well as the measured diffusion coefficients of ClO_2^- as a function of temperature, are summarized in Table 2. Determinations of k_{el} were made between 10 and 30 °C in 5 °C increments, and the results are summarized in Table 3. A plot of ln k_{el} vs $1/T$ is shown in Figure 7, and the resulting activation free energy and preexponential factor (25 ± 3.1 kJ/mol and 350(+900/−250) cm/s) are in excellent agreement with the rotating disk method.

TABLE 2: Kinematic Viscosities (ν) of 1.0 M KNO_3 and Diffusion Coefficients (D) of ClO_2^- as a Function of Temperature

T (K)	ν (cm²/s)	$D_{ClO_2^-}$ (cm²/s)
283	0.0133 ± 0.0002	(8.8 ± 0.07) × 10^{-6}
288	0.0118 ± 0.0001	(9.6 ± 0.08 × 10^{-6}
293	0.0106 ± 0.0001	(1.1 ± 0.01) × 10^{-5}
298	0.0095 ± 0.0001	(1.2 ± 0.03) × 10^{-5}
303	0.00873 ± 0.0001	(1.4 ± 0.03) × 10^{-5}

TABLE 3: Heterogeneous Charge Transfer Rate Parameters for ClO_2^-/ClO_2 in 1.0 M KNO_3 as a Function of Temperature Obtained from ac Voltammograms on a Au Electrode

T (K)	k_{el} (cm/s)	α
283	0.0077 ± 0.0005	0.49 ± 0.01
288	0.0090 ± 0.0009	0.49 ± 0.01
293	0.010 ± 0.0006	0.48 ± 0.01
298	0.014 ± 0.0009	0.50 ± 0.01
303	0.015 ± 0.0004	0.50 ± 0.01

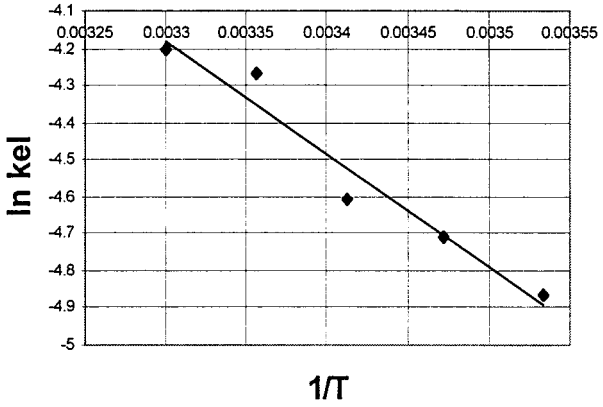

Figure 7. Plot of ln k_{el} vs $1/T$ for the ClO_2^-/ClO_2 redox couple at a Au electrode for data obtained using ac voltammetry.

Double-Layer Correction to k_{el}. Electron transfer does not occur between the reactant in bulk solution and the electrode but between the reactant in a precursor state and the electrode. Reactant must first be transported to the outer Helmholtz plane before electron transfer occurs. Since the potential drops off as a function of distance from the electrode surface, the applied potential is not equivalent to the potential experienced at the outer Helmholtz plane. This phenomenon is sometimes referred to as the Frumkin effect.[29,33] In the simplest case, the work required to form the precursor state is defined as the work required to bring the bulk reactant to the outer Helmholtz plane. Similarly, a successor state exists which directly precedes the bulk product. Equation 7 is the relation used to calculate these work terms, where Z = the charge on the redox species and ϕ_d = the potential at the outer Helmholtz plane.

$$w = ZF\phi_d \quad (7)$$

The Guoy−Chapman model of the electrochemical double layer is employed to estimate ϕ_d, and thereby the work required to form the precursor state from the bulk reactant w_p and the bulk product from the successor state w_s. In this model, the potential at distance x from the electrode surface is given by eq 8, where z = charge of electrolyte, e = elementary charge, ϕ =

TABLE 4: Standard and Corrected Heterogeneous Charge Transfer Rate Constants for the ClO_2^-/ClO_2 Redox Couple in 0.5, 1.0, and 1.5 M KNO_3

T (K)	k_{el} 0.5 M	k_{el} 1.0 M	k_{el} 1.5 M	k_{corr} 0.5 M	k_{corr} 1.0 M	k_{corr} 1.5 M
283	0.0074 ± 0.0002	0.0098 ± 0.0005	0.011 ± 0.0004	0.018	0.017	0.016
288	0.0090 ± 0.0003	0.010 ± 0.0004	0.012 ± 0.0008	0.022	0.017	0.017
293	0.010 ± 0.0004	0.013 ± 0.0009	0.016 ± 0.0005	0.024	0.022	0.023
298	0.012 ± 0.0004	0.015 ± 0.001	0.018 ± 0.001	0.029	0.026	0.026
303	0.015 ± 0.0009	0.019 ± 0.003	0.019 ± 0.003	0.036	0.032	0.027

TABLE 5. Heterogeneous Charge Transfer Rate Parameters for the ClO_2^-/ClO_2 Redox Couple in 1.0 M KNO_3 on a Rotating Disk Au Electrode in D_2O, and Corrected Heterogeneous Rate Constants in H_2O and D_2O and Their Ratios

T (K)	k_{el} D_2O (cm/s)	α D_2O	k_{corr} H_2O (cm/s)	k_{corr} D_2O (cm/s)	k_{H_2O}/k_{D_2O} corr
283	0.0072 ± 0.0002	0.50 ± 0.01	0.017	0.012	1.42
288	0.0091 ± 0.0006	0.56 ± 0.02	0.017	0.016	1.06
293	0.011 ± 0.0003	0.61 ± 0.01	0.022	0.019	1.16
298	0.012 ± 0.0006	0.59 ± 0.02	0.026	0.021	1.24
303	0.015 ± 0.0008	0.53 ± 0.02	0.032	0.026	1.23

potential at distance x, k = Boltzmann's constant, and ϕ_0 = applied potential.

$$\frac{\tanh\left(\frac{ze\phi}{4kT}\right)}{\tanh\left(\frac{ze\phi_0}{4kT}\right)} = e^{-\kappa x} \tag{8}$$

κ is given by eq 9, where n^0 = number concentration of supporting electrolyte, ϵ = static dielectric constant of the solution, and ϵ_0 = permittivity of vacuum.

$$\kappa = \left(\frac{2n^0z^2e^2}{\epsilon\epsilon_0 kT}\right)^{1/2} \tag{9}$$

In these calculations, ϕ_0 is set equal to the value of $E_{1/2}$ for the ClO_2^-/ClO_2 couple, x is taken as the average radius of a spherical approximation for ClO_2^- plus 1 H_2O diameter (4.2 Å), and ϵ is taken from the literature.[34] The average radius is given by $a = (l_x l_y l_z)^{1/3}$, where l_x, l_y, and l_z are equal to half the dimensions of the smallest box enclosing ClO_2^-. Consequently, k_{el} can be corrected for double-layer effects by using eq 10.

$$\ln k_{el} = \ln k_{corr} + \frac{(Z + \alpha)F\phi_d}{RT} \tag{10}$$

The rate k_{corr} represents the heterogeneous rate constant of the electron transfer process itself, noninclusive of the energy required to form the precursor and successor states. Table 4 lists observed and corrected heterogeneous rate constants for the ClO_2^-/ClO_2 redox couple in 0.5, 1.0, and 1.5 M KNO_3 obtained by the rotating disk method.

Heterogeneous Charge Transfer Rate Constants for the ClO_2^-/ClO_2 Redox Couple in D_2O. To test whether ClO_2^- exhibited stronger hydrogen bonding to solvent as compared to ClO_2, the rotating disk method was applied to determine heterogeneous charge transfer rate constants in D_2O. Weaver and co-workers have done similar work using metal cations and metal ammine and aquo complexes.[35,36] Unlike some of the metal complexes studied previously, the ClO_2^-/ClO_2 system will not undergo isotopic exchange with D_2O. Therefore, any anomalies observed can be attributed solely to solvent effects. In systems where differential hydrogen bonding effects for species of different charge are substantial, the ratio of the heterogeneous rate constants in H_2O and D_2O are much higher than the Marcus-solvent dielectric continuum model prediction of 1.06. In the ClO_2^-/ClO_2 system, no change in the formal potential was observed, and heterogeneous charge transfer rate constants were only slightly slower in D_2O. Table 5 summarizes the rate constants obtained in D_2O, as well as those corrected for double-layer effects for both H_2O and D_2O. The observed ratios k_{H_2O}/k_{D_2O} are in all cases much lower than those observed for metal complexes, and it suggests that the dielectric continuum treatment of outersphere solvation is a reasonable approximation for the ClO_2^-/ClO_2 couple.[35,36]

TABLE 6: Heterogeneous Charge Transfer Rates for the ClO_2^-/ClO_2 Redox Couple in 1.0 M KNO_3 at Pt and Glassy Carbon as a Function of Temperature

T (K)	Pt k_{el} (cm/s)	glassy carbon k_{el} (cm/s)
283	0.0084 ± 0.0007	0.0031 ± 0.00005
288	0.0091 ± 0.002	0.0037 ± 0.00006
293	0.011 ± 0.002	0.0048 ± 0.0004
298	0.014 ± 0.003	0.0079 ± 0.001
303	0.016 ± 0.003	0.0086 ± 0.002

Heterogeneous Charge Transfer Rate Constants for the ClO_2^-/ClO_2 Redox Couple at Pt and Glassy Carbon. Heterogeneous rate constants were measured on different electrode surfaces to determine whether electron transfer occurs via an inner- or outersphere mechanism. If an innersphere mechanism is operative, then the electron transfer rate constant should vary greatly on different electrode surfaces.[33] As noted earlier, the Pt electrode eventually suffered from surface fouling, which retarded the rate of electron transfer. The long scan times necessary in ac voltammetry measurements resulted in surface fouling on the time scale of each individual experiment. Therefore, it was impossible to obtain reproducible ac voltammograms, even after reductive pretreatment. Others have noted that reproducible ac voltammograms are highly dependent on the cleanliness of the electrode surface.[37] Unlike ac voltammetry, rotating disk experiments can be performed more rapidly. Therefore, heterogeneous rate constants for the ClO_2^-/ClO_2 redox couple on Pt were gathered using this technique.

The rate of electron transfer as a function of temperature is shown in Table 6 for both Pt and glassy carbon. For prereduced Pt, it can be seen that the rates are similar to those obtained at a Au electrode. However, the heterogeneous rate constants at glassy carbon are considerably slower. In general, electron transfer to and from glassy carbon is slower than on metal electrode surfaces, and only extensive polishing and pretreatment schemes can remedy this problem.[38] As a further test for adsorbed species that might lead to an innersphere pathway, double potential step chronocoulometry was performed. The resulting Anson plots indicated undetectable surface adsorption by the redox active species.[29] Thus, the electron transfer in the ClO_2^-/ClO_2 system appears to be similar to that observed for other outersphere redox species.

Digital Simulation of Cyclic Voltammograms using Measured Rate Constants. To further test the consistency of the heterogeneous rate parameters, digital simulations of cyclic voltammograms were performed using transfer coefficients, heterogeneous rate constants, and diffusion coefficients obtained from the ac voltammetry and rotating disk measurements. These simulated voltammograms were compared with those measured on Au, Pt, and glassy carbon electrodes. As can be seen in Figures 8−10 the simulated and experimental voltammograms correspond well.

Discussion

Sluggish electron transfer kinetics in the ClO_2^-/ClO_2 system was surprising given the simplicity of the redox couple. To understand the possible reasons for slow heterogeneous electron transfer, Marcus theory[39] was applied. The energy involved in electron transfer reactions at electrodes can be separated into three components: innersphere reorganization (internal changes in bond lengths and bond angles), outersphere reorganization (solvent reorganization), and reactant and product work terms (work required to transport reactant and product to and from the point where electron transfer can occur). These terms can be evaluated individually and compared to experimental values. Additionally, the variables contributing to the preexponential factor were analyzed.

Innersphere Reorganization Term for the ClO_2^-/ClO_2 Redox Couple. Chlorite has a bond angle of 111° and a Cl−O bond distance of 1.57 Å, whereas ClO_2 has a bond angle of 117.5° and a Cl−O bond distance (r) of 1.47 Å.[40] Therefore, the transformation from ClO_2^- to ClO_2 involves an angle (α') expansion of 6.5° and two bond contractions of 0.10 Å. The innersphere term corresponding to this transformation can be calculated by plotting the valence force field potential energy surfaces (determined by vibrational spectroscopy), as given in eq 11, where k_r and $k_{\alpha'}$ are the bond stretching and bending force constants, respectively, and r_o is the equilibrium bond distance.[40]

$$E = k_r \Delta r^2 + \frac{1}{2} k_{\alpha'} r_o^2 \Delta \alpha'^2 \qquad (11)$$

The minimum intersection along the totally symmetric pathway between the two surfaces yields the innersphere reorganization energy required for the electron transfer to take place. This analysis yields an energy barrier of 9.1 kJ/mol. Additionally, the theoretical transfer coefficient $\alpha = 0.45$ was calculated by analyzing the mean slopes of the potential energy surfaces at the point of intersection.[29] Figure 11 shows the intersection of the two potential energy surfaces.

Outersphere Reorganization Term for the ClO_2^-/ClO_2 Redox Couple. The outersphere reorganization term can be estimated by treating the solvent as a dielectric continuum as described by Marcus.[39] The validity of this approximation is supported by the small deuterium isotope effect observed for k_{el}, which argues against specific hydrogen bonding strongly favoring one redox component. Equation 12 was used to estimate the solvent reorganization energy, where e = elementary charge in esu, a = reactant radius, R_e = twice the reactant−electrode distance, ϵ_{op} = optical or infinite dielectric constant, and ϵ_s = static dielectric constant.[41]

$$\Delta G^*_{o.s.} = \frac{e^2}{8}\left(\frac{1}{a} - \frac{1}{R_e}\right)\left(\frac{1}{\epsilon_{op}} - \frac{1}{\epsilon_s}\right) \qquad (12)$$

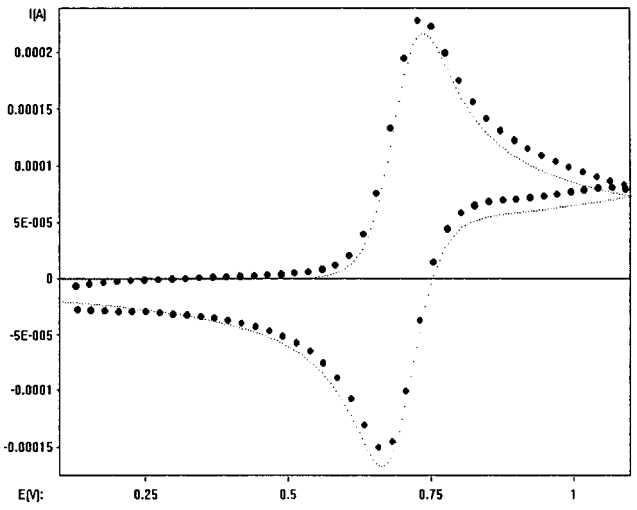

Figure 8. Digitally simulated (·) and experimental (●) cyclic voltammograms for the ClO_2^-/ClO_2 redox couple on Au at 25 °C. Simulation parameters: $[ClO_2^-] = 0.0055$ M, $D = 1.2 \times 10^{-5}$ cm²/s, scan rate = 0.050 V/s, $A = 0.1963$ cm², $E_{1/2} = 0.701$ V, $\alpha = 0.49$, $k_{el} = 0.015$ cm/s.

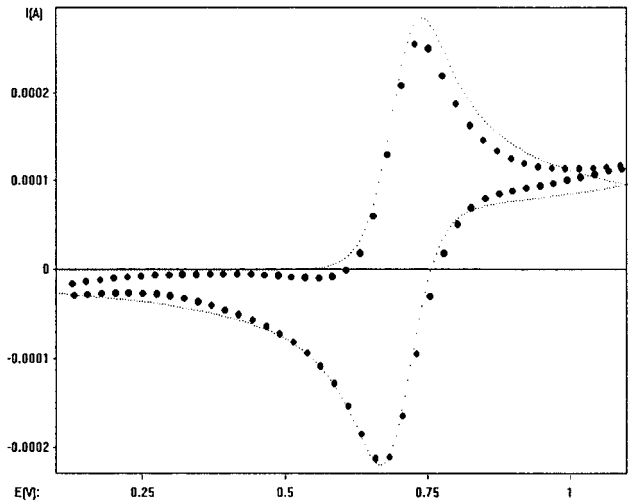

Figure 9. Digitally simulated (·) and experimental (●) cyclic voltammograms for the ClO_2^-/ClO_2 redox couple on Pt at 25 °C. Simulation parameters: $[ClO_2^-] = 0.0072$ M, $D = 1.2 \times 10^{-5}$ cm²/s, scan rate = 0.050 V/s, $A = 0.1963$ cm², $E_{1/2} = 0.7035$ V, $\alpha = 0.49$, $k_{el} = 0.016$ cm/s.

The smallest box enclosing ClO_2^-, as determined by molecular modeling, can be used to determine the average radius of a spherical approximation as described previously. Additionally, three possible radii can be obtained from the dimensions of the box, which refer to the different possible orientations of the ClO_2^- molecule with respect to the electrode surface. The reactant−electrode distance was taken to be one of the four reactant radii plus 1 H_2O diameter. The optical and static dielectric constants were taken from the literature, and for 1.0 M KNO_3, they had values of 5.51 and 68.59, respectively, at 25 °C.[34] Debye introduced the simplification of using the square of the refractive index as being an approximation to the optical dielectric constant for gases, which some investigators have taken to apply in solution electrochemical studies. However, in polar liquids, Debye states that the dielectric constant at high frequencies of perturbation, i.e., the infinite dielectric constant, is the true optical dielectric constant.[42] Using the latter values, the outersphere reorganization term was calculated to range between 10.9 and 26.3 kJ/mol, with a value of 18.8 kJ/mol for

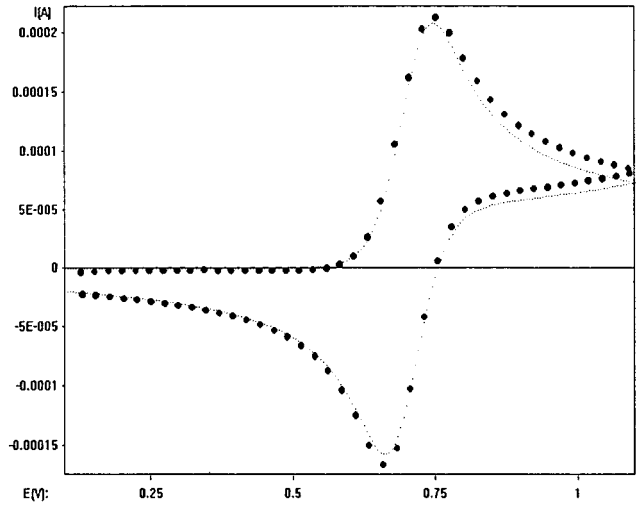

Figure 10. Digitally simulated (·) and experimental (●) cyclic voltammograms for the ClO_2^-/ClO_2 redox couple on glassy carbon at 25 °C. Simulation parameters: $[ClO_2^-] = 0.0054$ M, $D = 1.2 \times 10^{-5}$ cm²/s, scan rate = 0.050 V/s, $A = 0.1963$ cm², $E_{1/2} = 0.704$ V, $\alpha = 0.49$, $k_{el} = 0.0079$ cm/s.

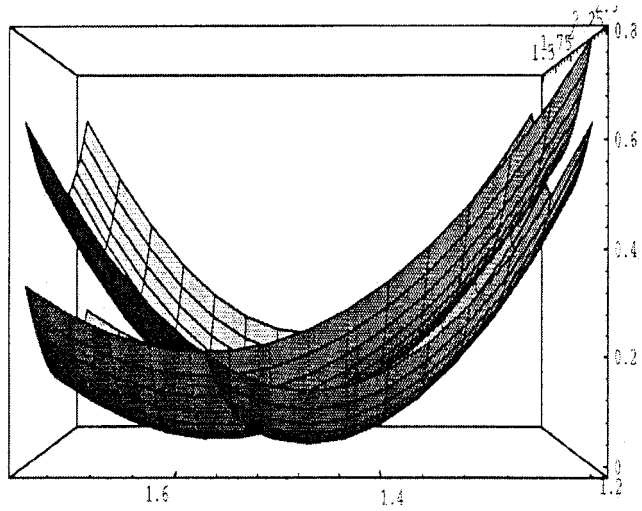

Figure 11. Plot showing the intersection of the valence force field potential energy surfaces for ClO_2^- and ClO_2.

the spherical approximation of the reactant radius. If one used the refractive index estimate ($n = 1.342$ for 1.0 M KNO_3), the value would range between 35.2 and 85.2 kJ/mol, with a value of 49.9 kJ/mol for the spherical approximation of the reactant radius. The experimental measurement of the infinite dielectric constant involves an extrapolation, and the values from ref 34 should be used with caution. Stanbury reports an outersphere reorganization energy of 32.7 kJ/mol for the self-exchange reaction between ClO_2^- and ClO_2, obtained by subtraction of the innersphere reorganization energy from the total activation barrier (work terms were neglected).[40] For an electrochemical reaction, the outersphere reorganization energy would be one-half this value, or 16.4 kJ/mol, which agrees better with the calculation using the experimentally estimated infinite dielectric constant. The other possible concern is that our estimate of the reactant−electrode distance is incorrect. If one assumes that the outersphere reorganization energy is 16.4 kJ/mol, uses the spherical approximation for the reactant radius, and instead uses the refractive index estimate for ϵ_{op}, then the reactant−electrode distance would have to be 1.68 Å for agreement. This reactant−electrode distance would require an innersphere mechanism (i.e. no water molecules between the reactant and the electrode). An innersphere mechanism seems unlikely given the slow rate of electron transfer, relative lack of influence of electrode material on rate of electron transfer, and lack of detectable adsorption from the Anson plots. The experimentally estimated dielectric constant at infinite frequency appears to be the better choice, even though its use is not common among the practitioners of Marcus Theory.

Reactant and Product Work Terms. The Guoy−Chapman model was used to estimate double-layer corrections (eqs 7−9). The outer Helmholtz plane is estimated to be the spherical approximation average radius of ClO_2^- plus one H_2O diameter as previously calculated. The dielectric constant for a 1.0 M KNO_3 solution at 25 °C is 68.59.[34] Since the charge on the product (ClO_2) is zero, its work term is also zero. For the reactant (ClO_2^-), the work term from Guoy−Chapman theory is −2.3 kJ/mol (negative because the positively charged electrode attracts the anion).

Free Energy Barriers to Electron Transfer for the ClO_2^-/ClO_2 Redox Couple. With the innersphere, outersphere, and work terms estimated, the theoretical free energy of activation $\Delta G^{\ddagger}$ for the electron transfer process for ClO_2^-/ClO_2 can be calculated. The stepwise calculation of $\Delta G^{\ddagger}$ is given in eqs 13−16.[33]

$$\Delta G^*_{int} = \Delta G^*_{i.s.} + \Delta G^*_{o.s.} \tag{13}$$

$$\Delta G^0_{et} = F(E - E^0) + (w_s - w_p) \tag{14}$$

$$\Delta G^* = \Delta G^*_{int} + \alpha_{et}\Delta G^0_{et} \tag{15}$$

$$\Delta G^{\ddagger} = \Delta G^* + w_p \tag{16}$$

Equation 13 gives the intrinsic barrier for the electron transfer step as the sum of the inner- and outersphere reorganization terms. For the ClO_2^-/ClO_2 system, ΔG^*_{int} is calculated to be 27.9 kJ/mol. Equation 14 is the free energy of electron transfer, where w_s is the work term of the successor state, and w_p is the work term of the precursor state. For the ClO_2^-/ClO_2 couple at the formal potential, $\Delta G^0_{et} = 2.3$ kJ/mol, due to the precursor state of ClO_2^-. Equation 15 yields the activation energy for the elementary step, i.e., the oxidation of the precursor ClO_2^- state. It is the sum of the intrinsic barrier for the electron transfer step and the free energy of electron transfer multiplied by the theoretical transfer coefficient $\alpha = 0.45$. It has a value of 29.0 kJ/mol. Last, $\Delta G^{\ddagger}$ equals the sum of the activation energy for the elementary step and the work term for the precursor state. For the ClO_2^-/ClO_2 system, the calculated value is 26.7 kJ/mol. This result is well within experimental error of the measured $\Delta G^{\ddagger}$ (eq 4) of 25 ± 3.3 kJ/mol. A free energy-reaction coordinate diagram with the calculated activation barriers is shown in Figure 12.

Preexponential Factor. The semiclassical expression for electrochemical reactions in eq 4 includes several preexponential terms. The reaction zone thickness δr is approximately 1 Å.[43] The nuclear tunneling factor is generally set equal to 1.[33] The remaining terms, ν_n (nuclear frequency factor) and κ_{el}^0 (electronic transmission coefficient) are less well defined. The nuclear frequency factor can be estimated by the formula given in eq 17, where ν_{os} = outershell solvent frequency of motion and $\nu_{is,s}$ = innershell vibration frequency of the symmetric Cl−O stretch, $\nu_{is,b}$ = innershell vibration frequency of the symmetric O−Cl−O bend, $\Delta G^*_{i.s.,s}$ = the stretching component of the internal reorganization energy, and $\Delta G^*_{o.s.,b}$ = the bending component of the internal reorganization energy.[33,44]

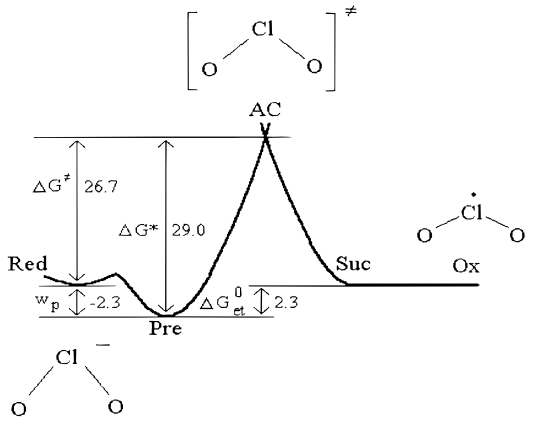

Figure 12. Free energy-reaction coordinate profile displaying free energy barriers (kJ/mol) in the oxidation of ClO_2^- to ClO_2.

$$\nu_n = \left(\frac{\nu_{os}^2 \Delta G^*_{o.s} + \nu_{is,s}^2 \Delta G^*_{i.s.,s} + \nu_{i.s.,b}^2 \Delta G^*_{i.s.,b}}{\Delta G^*_{o.s.} + \Delta G^*_{i.s.,s} + \Delta G^*_{i.s.,b}} \right) \quad (17)$$

The value of ν_{os} can be determined from the longitudinal relaxation time τ_L given by eq 18, where τ_D = Debye relaxation time determined from dielectric loss measurements.[33] All the necessary values for this calculation were obtained from ref 34. The outershell frequency factor is then calculated from eq 19.

$$\tau_L = \frac{\epsilon_\infty}{\epsilon_s} \tau_D \quad (18)$$

$$\nu_{os} = \tau_L^{-1} \left(\frac{\Delta G^*_{o.s.}}{4\pi kT} \right)^{1/2} \quad (19)$$

The calculation for τ_L gave a value of 6.20×10^{-13} s, and the corresponding value for ν_{os} at 298 K was 1.12×10^{12} s^{-1}. The innershell vibration frequency can be estimated using the symmetric stretching and bending frequencies of ClO_2^- and ClO_2 available from vibrational spectroscopy by using eq 20.[45]

$$\nu_{is,s/b}^2 = \frac{2\nu^2_{ClO_2^-,s/b}\nu^2_{ClO_2,s/b}}{\nu^2_{ClO_2^-,s/b} + \nu^2_{ClO_2,s/b}} \quad (20)$$

This calculation for the nuclear frequency factor ν_n yields 1.50×10^{13} s^{-1}. The electronic transmission coefficient, κ_{el}^0, is a measure of the adiabaticity of the electron transfer, and it equals 1 for an adiabatic pathway. Generally, it is assumed that electron transfer from metal electrodes proceeds adiabatically.[33] If this assumption is made with the system under study, the theoretical preexponential factor is calculated to be 1.5×10^5 cm/s. Obviously, there is a large discrepancy between the experimental and theoretical preexponential factors which can be rectified by assuming a nonadiabatic pathway ($\kappa_{el}^0 = 2.1 \times 10^{-3}$), a much lower nuclear frequency factor, or a combination of the two.

Self-Exchange Rate Constant for the ClO_2^-/ClO_2 Couple. Marcus theory predicts that the heterogeneous charge transfer rate constant at $E°$ (corrected for double-layer effects) is related to the chemical self-exchange rate constant by the expression given in eq 21, where k_{corr} and k_{ex} have units of cm/s and M^{-1} s^{-1}, respectively.[39]

$$\frac{k_{corr}}{Z_{el}} = \left(\frac{k_{ex}}{Z_{ex}} \right)^{1/2} \quad (21)$$

In this equation, Z_{el} and Z_{ex} are collision frequencies; however, adiabaticity is an implicit assumption. Instead, Z_{el} and Z_{ex} can be replaced by the encounter preequilibrium terms A_e and A_h, in eq 22 and eq 23, where the subscripts *e* and *h* refer to electrochemical and homogeneous reactions, respectively. In the expression for A_h, N = Avogadro's number and r' = the distance between the centers of ClO_2^- and ClO_2 when they are just touching.[43]

$$A_e = \delta r \, \kappa^0_{el} \nu_n \Gamma_n \quad (22)$$

$$A_h = 4\pi N r'^2 \, \delta r \, \kappa^0_{el} \, \nu_n \Gamma_n \quad (23)$$

A molecular model has been used to study the electrochemical reduction of Fe^{3+} to Fe^{2+} in aqueous solution at a Pt electrode, and a nonadiabatic value of 5×10^{-4} was found for κ_{el}^0.[46] This value is similar to our experimentally implied value of 2.1×10^{-3} for ClO_2^-/ClO_2 which leads to $A_e = 310$ cm/s. An experimental κ_{el}^0 for the homogeneous solution self-exchange reaction of Fe^{3+} and Fe^{2+} has been determined as 1.37×10^{-2}.[47] Using this value as an estimate for the homogeneous solution ClO_2^-/ClO_2 self-exchange κ_{el}^0, A_h is calculated as 9.7×10^9 M^{-1} s^{-1}. Subsequently, k_{ex} is estimated as 68 M^{-1} s^{-1}, which is in good agreement with those (27−1100 M^{-1} s^{-1}) obtained by homogeneous reaction studies.[40]

Conclusions

The heterogeneous electron transfer rate constants for the ClO_2^-/ClO_2 redox couple have been measured by ac voltammetry and rotating disk electrochemistry and verified by cyclic voltammetry. Chlorite is one of the few simple anions that exhibits a chemically reversible couple in aqueous solution. The measured heterogeneous charge transfer rate constant at 25 °C was 0.015 ± 0.001 cm/s with a $\Delta G^‡$ for the redox process of 25 ± 3.3 kJ/mol and a preexponential factor of 310(+900/−230) cm/s at a gold electrode. Comparable rate constants obtained at Au and reduced Pt electrodes suggest that the oxidation occurs via an outersphere mechanism. Changing the solvent from H_2O to D_2O resulted in no significant change in formal potential or heterogeneous rate constant.

The sluggish electrode kinetics are attributed to the sizable $\Delta G^‡$ and the small measured preexponential factor which is less than the theoretical value by over 2 orders of magnitude. The small measured preexponential factor suggests that electron transfer is nonadiabatic. If one accepts the nonadiabatic explanation, then it also removes the discrepancy between self-exchange calculations using heterogeneous and homogeneous rate data. Previous work has elucidated the shortcomings of the Marcus self-exchange relationship when applied to electrochemical rate data.[48,49] This apparent failure of Marcus theory may be due to greater nonadiabaticity in certain electrochemical reactions. It has been suggested that some redox species are unable to approach the electrode surface as closely as others.[50] Therefore, the nonadiabaticity may reflect the weak overlap between orbitals of the redox species and electrode surface due to the reactant-electrode separation.

It is noteworthy that the heterogeneous rate of oxidation of NO_2 to NO_2^+ was reported as 0.017 ± 0.003 cm/s in dichloromethane solvent.[51] It is possible that sluggish heterogeneous electron transfer rates are characteristic of bent triatomic molecules due to the importance of both the inner- and outersphere reorganization energies as well as the nonadiabaticity of electron transfer.

Acknowledgment. It is a pleasure to contribute this article to the special issue of the *Journal of Physical Chemistry* honoring Kent Wilson's pioneering experimental and theoretical scientific contributions in reaction dynamics. Support for this research by the National Science Foundation is gratefully acknowledged. We thank Nancy Logan of Sterling Pulp Chemicals, and Cliff Kubiak and Mike Sailor for helpful discussions.

References and Notes

(1) Miller, G. W. *An Assessment of Ozone and Chlorine Dioxide Technologies for Treatment of Municipal Water Supplies: Executive Summary*; Miller, G. W., Ed.; Environmental Protection Agency, Office of Research and Development, Municipal Environmental Research Laboratory: Cincinnati, Ohio, 1978; p 6.

(2) Symons, J. M. *Ozone, Chlorine Dioxide, and Chloramines as Alternatives to Chlorine for Disinfection of Drinking Water: State-of-the-Art*; Symons, J. M., Ed.; Environmental Protection Agency, Office of Research and Development, Water Supply Research Division: Cincinnati, Ohio, 1978; p 84 (revised in April).

(3) Morissette, C.; Prevost, M.; Langlais, B. *J. Water Supply Res. Technol.-Aqua* **1996**, *45*, 232.

(4) Owusuyaw, J.; Toth, J. P.; Wheeler, W. B.; Wei, C. I. *J. Food Sci.* **1990**, *55*, 1714.

(5) Richardson, S. D.; Thruston, A. D.; Collette, T. W.; Patterson, K. S.; Lykins, B. W.; Majetich, G.; Zhang, Y. *Environ. Sci. Technol.* **1994**, *28*, 592.

(6) Larson, R. A.; Weber, E. J. *Reaction Mechanisms in Environmental Chemistry*; Lewis Publishers: Boca Raton, 1994.

(7) Li, J. W.; Yu, Z. B.; Cai, X. P.; Gao, M.; Chao, F. H. *Water Res.* **1996**, *30*, 2371.

(8) Masschelein, W. J. *Chlorine Dioxide: Chemistry and Environmental Impact of Oxychlorine Compounds*; Ann Arbor Science Publishers: Ann Arbor, 1979.

(9) Farr, R. W.; Walton, C. *Infect. Control Hosp. Epidemiol.* **1993**, *14*, 527.

(10) DePalo, T.; Atti, M.; Bellantuono, R.; Giordano, M.; Caringella, D. *Blood Purif.* **1997**, *15*, 188.

(11) Hamilton, E.; Seal, D.; Hay, J. *J. Hosp. Infect.* **1996**, *32*, 156.

(12) Oliver, S. P.; King, S. H.; Torre, P. M.; Schull, E. P.; Dowlen, H. H.; Lewis, M. J.; Sordillo, L. M. *J. Dairy Sci.* **1989**, *72*, 3091.

(13) Tsai, L. S.; Higby, R.; Schade, J. *J. Agric. Food Chem.* **1995**, *43*, 2768.

(14) Walker, J. T.; Mackerness, C.; Mallon, D.; Makin, T.; Williets, T.; Keevil, C. *J. Ind. Microbiol.* **1995**, *15*, 384.

(15) Solomon, K.; Bergman, H.; Huggett, R.; Mackay, D.; McKague, B. *Pulp Paper Can.* **1996**, *97*, 35.

(16) Pryke, D. C.; Winter, P.; Bouree, G. R.; Mickowski, C. *Pulp Paper Can.* **1994**, *95*, 40.

(17) Daube, A. K.; Karim, M. R.; Dimmel, D. R.; McDonough, T. J.; Banerjee, S. *Environ. Sci. Technol.* **1992**, *26*, 1324.

(18) Liyanage, L. R. J.; Finch, G. R.; Belosevic, M. *Ozone Sci. Eng.* **1997**, *19*, 409.

(19) Korich, D. G.; Mead, J. R.; Madore, M. S.; Sinclair, N. A.; Sterling, C. R. *Appl. Environ. Microbiol.* **1990**, *56*, 1423.

(20) Vaida, V.; Simon, J. D. *Science* **1995**, *268*, 1443.

(21) Gordon, G.; Kieffer, R. G.; Rosenblatt, D. H. In *Progress in Inorganic Chemistry*; Lippard, S. J., Ed.; Wiley: New York, 1972; Vol. 15, pp 201−286.

(22) Hull, L. A.; Davis, G. T.; Rosenblatt, D. H.; Williams, H. K. R.; Weglein, R. C. *J. Am. Chem. Soc.* **1967**, *89*, 1163.

(23) Hull, L. A.; Giordano, W. P.; Rosenblatt, D. H.; Davis, G. T.; Mann, C. K.; Milliken, S. B. *J. Phys. Chem.* **1969**, *63*, 2147.

(24) Rosenblatt, D. H.; Hull, L. A.; Luca, D. C. D.; Davis, G. T.; Weglein, R. C.; Williams, H. K. R. *J. Am. Chem. Soc.* **1967**, *89*, 1158.

(25) Schwarzer, O.; Landsberg, R. *J. Electroanal. Chem.* **1967**, *14*, 339.

(26) Raspi, G.; Pergola, F. *J. Electroanal. Chem.* **1969**, *20*, 419.

(27) Masschelein, W. J.; Denis, M.; Ledent, R. *Anal. Chim. Acta* **1979**, *107*, 383.

(28) Nakareseisoon, S.; Tachiyashiki, S.; Benga, J.; Pacey, G. E.; Gordon, G. *Anal. Chim. Acta* **1988**, *204*, 169.

(29) Bard, A. J.; Faulkner, L. R. *Electrochemical Methods: Fundamentals and Applications*; Wiley: New York, 1980.

(30) Smith, D. E. In *Electroanalytical Chemistry*; Bard, A. J., Ed.; Marcel Dekker: New York, 1966; Vol. 1, pp 132−134.

(31) Breyer, B.; Bauer, H. H. *Alternating Current Polarography and Tensammetry*; Wiley: New York, 1963; p 63.

(32) Gilman, S. In *Electroanalytical Chemistry*; Bard, A. J., Ed.; Marcel Dekker: New York, 1967; Vol. 2, pp 111−192.

(33) Weaver, M. J. In *Comprehensive Chemical Kinetics*; Compton, R. G., Ed.; Elsevier: New York, 1987; Vol. 27, pp 1−60.

(34) Barthel, J.; Neueder, R. *Electrolyte Data Collection, Part 2: Dielectric Properties of Water and Aqueous Solution*, Chemistry Data Series DECHEMA: Frankfurt/Main, Germany, 1995; Vol. 12, pp 266−269.

(35) Weaver, M. J.; Tyma, P. D.; Nettles, S. M. *J. Electroanal. Chem.* **1980**, *114*, 53.

(36) Weaver, M. J.; Nettles, S. M. *Inorg. Chem.* **1980**, *19*, 1641.

(37) Fu, Y.; Swaddle, T. W. *J. Am. Chem. Soc.* **1997**, *119*, 7137.

(38) Kinoshita, K. *Carbon: Electrochemical and Physicochemical Properties*; Wiley: New York, 1988; pp 228−231, 251−258.

(39) Marcus, R. A. *J. Chem. Phys.* **1965**, *43*, 679.

(40) Stanbury, D. M.; Lednicky, L. A. *J. Am. Chem. Soc.* **1984**, *106*, 2847.

(41) The original Marcus equation has been simplified for a one-electron electrode reaction and setting $m = 0.5$, meaning the activated complex has a structure intermediate between the reactant and product. This equation yields the solvent reorganization energy between the reactant and the transition state. In the literature, λ represents the total vertical reorganization energy (outer- and innersphere). The total outersphere reorganization energy between reactant and product λ_{os} would be calculated by setting $m = 1$, and the result would be 4 times the value given by eq 11. Therefore, $\Delta G_{o.s.}$ equals $^1/_4\lambda_{os}$. The same conclusion is reached by considering the mathematical expression for the intersection of two parabolic curves with zero y-displacement. See Calvo, E. J. In *Comprehensive Chemical Kinetics*; Bamford, C. H.; Compton, R. G., Eds.; Elsevier: New York, 1986; Vol. 26, Chapter 1, pp 48−57.

(42) Debye, P. *Polar Molecules*; Dover: New York, 1960; pp 42−44, 89−95.

(43) Hupp, J. T.; Weaver, M. J. *J. Electroanal. Chem.* **1983**, *152*, 1.

(44) The innershell stretching and bending vibrations are taken as the average of ClO_2^- and ClO_2.

(45) Hupp, J. T.; Weaver, M. J. *J. Phys. Chem.* **1985**, *89*, 2795.

(46) Rose, D. A.; Benjamin, I. *J. Chem. Phys.* **1994**, *100*, 3545.

(47) Guan, D.; Bu, Y.; Deng, C. *J. Mol. Struct.* **1997**, *417*, 145.

(48) Saji, T.; Yamada, T.; Aoyagui, S. *J. Electroanal. Chem.* **1975**, *61*, 147.

(49) Saji, T.; Maruyama, Y.; Aoyagui, S. *J. Electroanal. Chem.* **1978**, *86*, 219.

(50) Weaver, M. J. *J. Phys. Chem.* **1980**, *84*, 568.

(51) Lee, K. Y.; Amatore, C.; Kochi, J. K. *J. Phys. Chem.* **1991**, *95*, 1285.